Proc. Natl. Acad. Sci. USA
Vol. 87, pp. 487–491, January 1990
Biophysics

Factors governing helical preference of peptides containing multiple α,α-dialkyl amino acids

[α-helix/α-aminoisobutyric acid (α-methylalanine)/emerimicin/peptaibol/x-ray crystallography]

GARLAND R. MARSHALL*†, EDWARD E. HODGKIN*, DAVID A. LANGS‡, G. DAVID SMITH‡, JANUSZ ZABROCKI§, AND MIROSLAW T. LEPLAWY§

*Department of Pharmacology, Washington University School of Medicine, Saint Louis, MO 63110; ‡Medical Foundation of Buffalo, Inc., Buffalo, NY 14203; and §Institute of Organic Chemistry, Politechnika, 90-924 Lodz, Poland

Communicated by Isabella L. Karle, June 22, 1989 (received for review July 28, 1988)

ABSTRACT **The presence of multiple α,α-dialkyl amino acids such as α-methylalanine (α-aminoisobutyric acid, Aib) leads to predominantly helical structures, either with α-helical or 3_{10}-helical hydrogen bonding patterns. The crystal structure of emerimicin-(1–9) benzyl ester (Ac-Phe-Aib-Aib-Aib-Val-Gly-Leu-Aib-Aib-OBzl) reported here shows essentially pure α-helical character, whereas other similar compounds show predominantly 3_{10}-helical structures. The factors that govern helical preference include the inherent relative stability of the α-helix compared with the 3_{10}-helix, the extra hydrogen bond seen with 3_{10}-helices, and the enhanced electrostatic dipolar interaction of the 3_{10}-helix when packed in a crystalline lattice. The balance of these forces, when combined with the steric requirements of the amino acid side chains, determines the relative stability of the two helical conformations under a given set of experimental conditions.**

The presence of α,α-dialkyl amino acids in microbial natural products, such as the peptaibol antibiotics, requires novel biosynthetic pathways to produce and incorporate these unusual amino acids in the face of the usual ribosomal mechanisms available for normal amino acids. This argues strongly for a special role related to function, one aspect of which may be their increased resistance to proteolytic degradation. Another aspect is the conformational restrictions imposed by these amino acids as first pointed out by Marshall and Bosshard (1, 2) and verified by others (3–7). While most work has focused on α-methylalanine (α-aminoisobutyric acid, Aib), α-ethylalanine (isovaline) has also been found to be a natural component of several peptaibol antibiotics (8, 9). In addition, chiral α,α-dialkyl amino acids, such as α-methylphenylalanine, have been incorporated into naturally occurring peptides in an effort to restrict their conformational freedom (10, 11).

From the Ramachandran plots published by Marshall and Bosshard in 1972 (1), the presence of an additional alkyl substituent on the α-carbon severely restricted the values of the torsional variables ϕ and ψ as compared with those available to normal amino acids. While the two major allowed conformational areas were associated with either right- or left-handed helical conformations (both α and 3_{10}), the calculation also revealed other sets of energetically feasible values for ϕ and ψ adjacent to the α,α-dialkyl residue associated with extended structures as well as turns. The effect on conformation of alkyl groups larger than methyl as substituents in α,α-dialkyl amino acids has also been investigated (11, 12). Despite the variety of conformations theoretically available to α,α-dialkyl amino acids, the impact of multiple substitutions of this type of amino acid on the overall conformation of a peptide is dramatic. The crystal structure of alamethicin (13), which contains 8 Aib residues out of 20, is predominantly α-helical, with NMR data (14) supporting a similar solution conformation in methanol. A review (15) of crystal structures of tri-, tetra-, and pentapeptides containing Aib indicates that all but one show characteristics of the 3_{10}-helix. Crystal structures of nine other, longer Aib-containing peptides show significant α-helical content (13, 16–23). Other Aib-containing peptides of 7 or more residues are predominantly 3_{10}-helices (24–29). Much conjecture regarding the factors determining either α- or 3_{10}-helical conformations has appeared (17, 18, 24, 25). Bosch *et al.* (17) and Toniolo *et al.* (24) correlated the length of the peptide with α-helical content. Karle *et al.* (18) correlated the content of Aib with the helix preference and stated that peptides of 7 or more residues containing 50% Aib residues favor the 3_{10}-helix, while those which are predominantly α-helical contain 30–35% Aib residues. Bavoso *et al.* (25) summarized the current empirical view "that Aib-rich peptides shorter than nine residues tend to fold into 3_{10}-helices" and "Aib-rich peptides longer than eight residues may adopt either the 3_{10}-helix or mixed $\alpha/3_{10}$-helices." Recently, Karle *et al.* (23) reported two crystalline forms of a decapeptide containing 3 Aib residues that switches from a predominantly α-helical hydrogen bonding pattern to a mixed $3_{10}/\alpha$-helical pattern depending on the solvent of crystallization. To gain insight into the factors determining the conformational preference resulting from the presence of multiple α,α-disubstituted amino acids, further work combining theoretical and experimental approaches was clearly needed. The crystal structure of the benzyl ester of emerimicin fragment 1–9, Ac-Phe-Aib-Aib-Aib-Val-Gly-Leu-Aib-Aib-OBzl, presented in this paper, emphasizes this problem and has stimulated a theoretical evaluation of factors governing the conformation of peptides containing multiple α,α-dialkyl amino acids.

EXPERIMENTAL

Crystal Structure. The benzyl ester of emerimicin-(1–9) was prepared in solution as part of a synthetic program involving the total syntheses of emerimicins III and IV (J. Z., A. Redlinski, M.T.L., J. B. Dunbar, Jr., and G.R.M., unpublished data). Single crystals of Ac-Phe-Aib-Aib-Aib-Val-Gly-Leu-Aib-Aib-OBzl were grown by slow evaporation of an ethanol/2-propanol mixture. The crystals ($C_{51}H_{77}N_9O_{11}\cdot 3H_2O$) belong to space group $P1$ with cell constants $a = 9.130 \pm 0.001$ Å, $b = 10.508 \pm 0.001$ Å, $c = 15.077 \pm 0.002$ Å, $\alpha = 96.73 \pm 0.01°$, $\beta = 99.29 \pm 0.01°$, and $\gamma = 89.09 \pm 0.01°$, one formula unit per cell ($Z = 1$), and a calculated density of 1.225 g/cm^3. A single crystal of dimensions 0.05 × 0.3 × 0.35 mm was mounted, and 5444 intensities

The publication costs of this article were defrayed in part by page charge payment. This article must therefore be hereby marked "*advertisement*" in accordance with 18 U.S.C. §1734 solely to indicate this fact.

Abbreviation: Aib, α-aminoisobutyric acid (α-methylalanine).
†To whom reprint requests should be addressed.

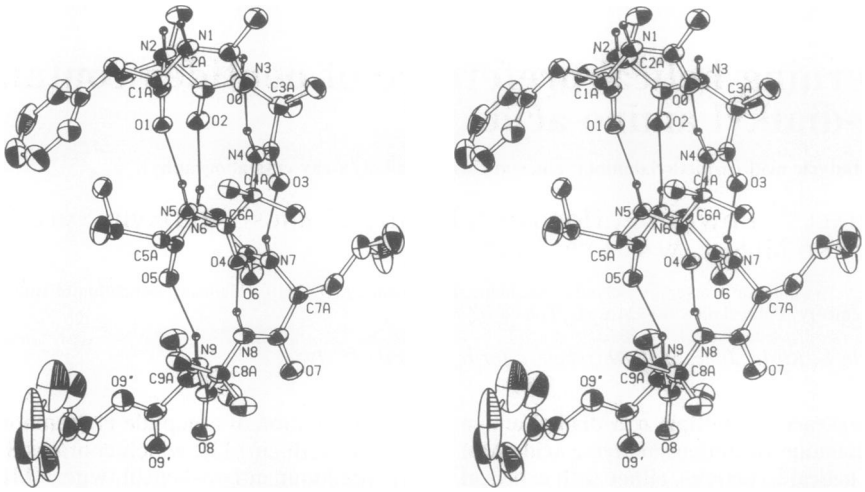

FIG. 1. Stereo drawing of the nonapeptide molecule. Amide nitrogen atoms are drawn with a radius of 0.08 Å; the remaining hydrogen atoms have been excluded for the sake of clarity. Hydrogen bonds are illustrated as thin bonds. Thermal ellipsoids are drawn at a 50% probability.

[maximum (sin θ)/λ = 0.546 Å^{-1}] were measured at 165 K with Ni-filtered Cu K_α radiation on a Nicolet P3 diffractometer using θ–2θ scans. The intensities were corrected for Lorentz and polarization factors but not for absorption (μ = 0.701 cm^{-1}) to yield a total of 3860 independent data. The variance of each structure factor was calculated according to the method of Blessing (30).

The structure was solved through the use of the direct methods program QTAN[¶] and refined by full matrix least-squares minimization of $\Sigma\, w(F_o - F_c)^2$ [where $w = 1/\sigma^2(F)$], treating the vibration of all nonhydrogen atoms anisotropically. The positions of the amide protons were determined from a ΔF map and were refined isotropically. The positions of the remaining protons were recalculated on the basis of idealized geometry at the end of each refinement cycle and were assigned an isotropic thermal parameter equal to 1.0 plus the equivalent isotropic B value of the atoms to which they were covalently bound. The final ΔF map did not disclose the positions of the hydrogen atoms of the water structure. During the course of the refinement, a $\delta(R)$ normal probability plot (31) suggested that 54 data had been incorrectly measured, and these were excluded from subsequent calculations. The refinement has converged at a residual of 0.037 and a weighted residual of 0.052 for the 3806 data used in the refinement (residual for all 3860 data is 0.038). The standard deviation of an observation of unit weight is 2.311. A stereo drawing illustrating the observed conformation is shown in Fig. 1. Torsion angles describing the conformation of the main chain and side chains are listed in Table 1. The atomic coordinates and the equivalent isotropic thermal parameters for the nonhydrogen atoms are being deposited with the Cambridge Crystallographic Data Center. Until such time as the data are available from this source, these data as well as tables of observed and calculated structure factors, anisotropic thermal parameters, and the hydrogen atom coordinates and thermal parameters are available from the authors (G.D.S. or G.R.M.).

Molecular Modeling. SYBYL (Tripos Associates, Saint Louis, MO) molecular modeling software was used. A Ramachandran plot was generated for each of the pairs of backbone torsional angles (ϕ, ψ) associated with each amino acid residue. The rigid geometry approximation was used with the set of scaled van der Waals radii shown by Iijima *et al.* (32) to reproduce the experimental crystal data for proteins and peptides. For each gridpoint shown to be sterically allowed for Aib in the helical regions (ϕ = −40° to −70° and ψ = −20° to −60°), decamers of both Aib and Ala were generated with the ϕ, ψ values for each monomer set to the same values. Full geometry optimization with the AMBER (33) force field used the SYBYL program module MAXIMIN. To characterize possible helical structures, further minimizations of oligomers $(Aib)_n$ and $(Ala)_n$, where n = 1–15, were performed in order to separate the intrinsic, or length-dependent, stability from end effects. In addition, ϕ, ψ values were constrained in separate minimizations in order to map the potential surface for helix interconversion. Details of these extensive calculations will be published elsewhere (E.E.H., J. D. Clark, K. R. Miller, and G.R.M., unpublished data).

[¶]Langs, D. A. & DeTitta, G. T., Tenth International Congress of Crystallography, 1975, Amsterdam, abstr. 02.2-14.

RESULTS AND DISCUSSION

Emerimicin-(1–9) benzyl ester forms slightly more than two and one-half turns of continuous α-helix in the crystal, as evidenced from the hydrogen bonding pattern. The 5→1 hydrogen bonding pattern characteristic of an α-helix is seen between the acetyl carbonyl and the amide NH group of Aib-4, the Phe-1 carbonyl and the amide NH group of Val-5, the Aib-2 carbonyl and the amide NH group of Gly-6, the Aib-3 carbonyl and the amide NH group of Leu-7, the Aib-4 carbonyl and the amide NH group of Aib-8, and the Val-5 carbonyl and the amide NH group of Aib-9. The NH–O distances vary from 2.97 Å to 3.08 Å, while the H–O distances vary from 2.08 Å to 2.16 Å. Contacts consistent with a 3_{10}-helical pattern (4→1) also exist, but the H–O distances calculated from the geometries show that these contacts are not hydrogen bonds. The torsional angles that describe the conformation of the peptide are given in Table 1 and are consistent with an α-helical assignment, although the ϕ, ψ values of Val-5 (−76°, −28°), Gly-6 (−60°, −32°), and Leu-7 (−82°, −32°) are in the region associated with 3_{10}-helical structures. In addition, a familiar pattern seen with Aib residues at the C terminus also exists. Residue 9 has the opposite helical sense (left-handed) from the remainder of the helical structure (right-handed).

Additional intermolecular hydrogen bonds exist between the amide nitrogen of Phe-1 and the carbonyl oxygen of a symmetry-related Aib-8 residue (2.85 Å) and between the amide nitrogen of Aib-2 and the carbonyl oxygen of Aib-9 of the same symmetry-related molecule (3.08 Å). In this way, α-helical rods are established by head-to-tail hydrogen bond-

Table 1. Torsion angles that describe the conformation of the peptide backbone and the side chains

Angle	Angle value, degrees									
	Ac-0	Phe-1	Aib-2	Aib-3	Aib-4	Val-5	Gly-6	Leu-7	Aib-8	Aib-9
ϕ		−62	−51	−58	−55	−76	−60	−82	−54	55
ψ		−43	−57	−50	−52	−28	−32	−32	−38	48
ω	−174	180	−178	−171	−176	172	175	172	172	179
χ^1		179				−58		−63		
χ^2		88						177		

ing. These rods pack in a parallel fashion, a pattern seen before in crystals containing Aib residues in α-helical conformation. Due to the 5→1 hydrogen bonding pattern of the helix, the amide of Aib-3 and the carbonyl of Gly-6 and Leu-7 remain without hydrogen bond partners from peptide residues. The three water molecules associated with the crystal form a hydrogen bonding network between these groups and the carbonyl oxygen of Aib-4. Thus, each potential hydrogen bond donor forms at least one hydrogen bond to an acceptor.

The finding that this fragment of emerimicin is α-helical is surprising for several reasons. First is the known crystal structure (24, 29) of a protected emerimicin-(2–9), pBrBz-Aib-Aib-Aib-Val-Gly-Leu-Aib-Aib-OMe, which assumes a 3_{10}-helix. In effect, changing the N-terminal *p*-bromobenzoyl group to an acetylphenylalanyl group and the C-terminal methyl ester to a benzyl ester switches the preference, possibly by the introduction of one additional carbonyl at the N terminus for hydrogen bonding. In addition, both the peptide length of nine residues and the content of 55% Aib would argue against α-helical structure by the empirical generalizations (17, 18, 24, 25). The observation (27) of an almost perfect 3_{10}-helix in crystals of the decapeptide Boc-Aib-Pro-Val-Aib-Val-Ala-Aib-Ala-Aib-Aib-OMe, which contains 50% Aib, would argue that length and Aib content are not the crucial factors *per se*.

What is needed is a theoretical basis for understanding the relative stability of α- and 3_{10}-helical structures. Our evaluation of the Aib oligomer resulted in an α-helix with $\phi = -55.2°$, $\psi = -52.2°$, $\omega = 180.2°$ and a 3_{10}-helix with $\phi = -49.9°$, $\psi = -31.1°$, $\omega = 178.5°$. Detailed analysis showed an increased stability of ≈1.92 kcal/mol per residue for the isolated α-helix relative to the 3_{10}-helix for oligomers of Aib, as compared with the estimate of 0.3–3.6 kcal/mol per residue by Prasad and Sasisekharan (5). Based on the energy surface generated, the 3_{10}-helix was entropically stabilized by ≈1 kcal/mol per residue over the α-helix (E.E.H. and G.R.M., unpublished data). The enthalpic difference between the 3_{10}-helix and the α-helix was −2.38 kcal/mol per residue for similar oligomers of alanine, where previous workers (5) had estimated between −3.3 and −3.6 kcal/mol per residue. These calculations are consistent with the small number of observations of 3_{10}-helix in proteins (34) as well as the increased probability of 3_{10}-helix with increased content of Aib residues.

A 3_{10}-helix makes an additional hydrogen bond for the same length peptide due to 4→1 hydrogen bonding rather than the 5→1 hydrogen bonding of the α-helix. In solution, a length of peptide is reached where the inherent increased stability of the α-helix dominates the energy contribution of the single additional hydrogen bond formed in a 3_{10}-helix. Although literature estimates show considerable variation, 7 kcal/mol was the average hydrogen bond strength in a simulation of liquid *N*-methylacetamide by Jorgensen and Swenson (35) using the OPLS force field (36). Hydrogen bond dissociation energies vary with the dielectric constant of the solvent, as seen in measurements of the heats of dissociation of dimeric acetic acid in various media (37). Our calculations *in vacuo* estimate the difference in end effects between the α- and 3_{10}-helix (primarily the extra hydrogen bond) to be 12 kcal/mol. These considerations imply modulation of the 3_{10}- to α-helix transition length by variation of the dielectric constant of the solvent. In short peptides, a 3_{10}-helix conformation is favored in solvents of low dielectric due to one additional hydrogen bond that can be satisfied. As the peptide length increases, the inherent stability of the α-helix compensates for the lost hydrogen bond and the α-helix becomes dominant in solution. Although the exact transition length will depend on the solvent and peptide sequence, we can estimate that most nonpolar solvents would require a length longer than seven residues for the α-helix to be favored.

Evidence from solution NMR studies support helix preference as a function of solvent polarity. Pentapeptides containing repetitive Aib-Ala or Aib-Val sequences showed three intramolecular hydrogen bonds in both C^2HCl_3 and $(C^2H_3)_2SO$, consistent with 3_{10}-helical structure (38). Heptapeptides of similar sequence had five hydrogen bonds in C^2HCl_3 (implying a 3_{10}-helix) but only four hydrogen bonds in the more polar $(C^2H_3)_2SO$, consistent with α-helical conformation (38). Balaram *et al.* (39) have reported that two decapeptides, Boc-Aib-Val-Aib-Aib-Val-Val-Val-Aib-Val-Aib-OMe and Boc-Aib-Leu-Aib-Aib-Leu-Leu-Leu-Aib-Leu-Aib-OMe (where Boc is *t*-butoxycarbonyl), show the presence of eight intramolecular hydrogen bonds in C^2HCl_3 but only seven hydrogen bonds in $(C^2H_3)_2SO$, consistent with a transformation from 3_{10}-helix to α-helix upon increasing the polarity of the solvent and decreasing the hydrogen bond strength. The absence of the assignment of the amide protons to specific residues in those studies leaves the helix-transformation interpretation of the data speculative, particularly due to the known propensity of these peptides to aggregate in a head-to-tail fashion. Whether the peptide is 3_{10}- or α-helical in the crystal, the formation of head-to-tail aggregates is a common feature. In general, only two of the unsatisfied hydrogen bonds at each end can be accommodated, leading to the inclusion of bridging water molecules as seen in the emerimicin-(1–9) crystal. While it is generally recognized that the acetyl group at the N terminus and the amino acid alcohol function both to eliminate the charged ends in membrane-active peptaibol antibiotics and to prevent exopeptidase degradation, they also serve to eliminate an unsatisfied hydrogen bond donor or acceptor at each end. The critical importance of residues with side chains capable of supplying hydrogen bonding groups to stabilize α-helical termini in proteins has only recently been recognized (40, 41).

While the factors that dictate helical preference in solution undoubtedly play a role in the crystal, intermolecular interactions become important and may actually dominate. The predicted enhanced stability of the α-helix in solution once a critical length is reached stands in contrast to the observation of 3_{10}-helical structure in crystals for numerous oligomers of Aib (29) as well as poly(Aib) (42, 43) itself. Sorensen *et al.* (44) analyzed two polymorphic crystal forms of poly(oxymethylene), with results indicating that intermolecular interactions within the crystal can modify the energy minima seen for the single molecule. One factor governing the crystal structures in poly(Aib) is an improved packing for the 3_{10}-helix as compared with the α-helix. This arises from the interdigita-

tion of the methyl side chains, which is accommodated by the 3_{10}-helix and an increased stabilization by van der Waals interaction, estimated at ≈0.35 kcal/mol per residue per helix–helix dimer interaction (E.E.H. and G.R.M., unpublished data). Another major aspect is electrostatic as the 3_{10}-helix has a smaller radius (1.9 versus 2.3 Å) than the α-helix and a similar dipole moment, 35.6 versus 36.8 debyes for the Aib decamer, which would result in a stronger electrostatic interaction during antiparallel helical stacking. That the dipoles associated with the amide bond can give significant interaction energies is clearly shown by the calculations of Hol and De Maeyer (45) and Furois-Corbin and Pullman (46). The electrostatic interaction energy between a helix and its neighbors was approximately −23 kcal/mol (44). If one assumes (16) the side chains to increase the diameter (the same as the distance between helices) of an α-helix to 9.4 Å (47), then the poly(Aib) 3_{10}-helix can be shown (42, 43) to have a shorter packing distance than expected between helices of 7.5 Å, due to interleaving of Aib side chains. The interaction energy between two adjacent antiparallel 3_{10}-helices would increase due to closer packing. The ≈20% reduction in distance would result in an increase of ≈73% in electrostatic energy because dipole–dipole interactions have an r^{-3} dependency. If the undecapeptide could pack as efficiently as a 3_{10}-helix, it would gain a maximum of −16.7 kcal/mol, or −1.52 kcal/mol per residue, in electrostatic stabilization. When the approximations made in the estimates and the inherent problem of dielectric with electrostatic calculations are taken into account, the value of −1.92 kcal/mol per residue for stabilization of α-helix over 3_{10}-helix is lower than the estimate of the electrostatic stabilization of the 3_{10}-helix over the α-helix in the crystal if one considers the entropic stabilization of the 3_{10}-helix (−1 kcal/mol per residue). The α-helical peptides containing multiple α,α-dialkyl amino acids seen in crystals, therefore, arise when the sequence of residues leads to unfavorable packing of the 3_{10}-helix. The correlation seen between Aib content and 3_{10}-helicity reflects the decreased bulk of the side chain. In the case of the α-helical undecapeptide mentioned above whose crystal structure was solved by Bosch *et al.* (16), the presence of the bulky *t*-butoxycarbonyl group and the Glu(OBzl) residue in the middle appears sufficient to prevent optimal packing of 3_{10}-helices. The replacement of the *p*-bromobenzoyl group by an acetylphenylalanyl group at the N terminus and the replacement of the methyl ester by the more bulky benzyl ester in emerimicin-(1–9) reported here were sufficient to prevent crystallization in the 3_{10}-helix as seen with the emerimicin-(2–9) analog. It is interesting that the solution data on an emerimicin-(2–9) fragment, Z-Aib-Aib-Aib-Val-Gly-Leu-Aib-Aib-OMe (where Z is benzyloxycarbonyl), were consistent with the presence of a right-handed α-helix (48) in trifluoroethanol, a hydrogen bonding solvent. In the case of Boc-(Aib-Ala-Leu)$_3$-Aib-OMe, the α-helix has been shown to predominate in the crystal by Karle *et al.* (20). The large leucine side chains, which repeat every third residue, would prevent the close association of antiparallel helices needed to stabilize the 3_{10}-helix in the crystal. Okuyama *et al.* (49) have reported the crystal structure of an octapeptide, Boc-Leu-Leu-Leu-Aib-Leu-Leu-Leu-Aib-OBzl, that packs α-helical columns in a parallel fashion. Sequence-dependent effects will further complicate this picture and may, in part, be responsible for the hybrid structures of α- and 3_{10}-helices. Certainly, the local packing constraints of amino acid side chains in 3_{10}- and α-helical conformations are important and account for the low α-helical propensity of β-forked residues such as valine and isoleucine. The crystal structure of Boc-Aib-Val-Aib-Aib-Val-Val-Val-Aib-Val-Aib-OMe by Karle *et al.* (21) has two molecules in the asymmetric unit, one as an α-helix and the other as a mixed α/3_{10}-helix, presumably to accommodate side-chain packing. The problem of side-chain packing may explain the extended conformation seen in oligomers of α,α-diethylglycine (12). α,α-Dialkyl amino acids preclude other energetically favorable intermolecular interactions such as β-sheet formation, as shown in studies comparing oligomers of α,α-dialkyl amino acids with oligomers of norvaline (50).

Parallel packing of α-helical peptides occurs (18, 19, 22, 23) and has also been reported with 3_{10}-helices (24). While true parallel arrays of α-helices are often seen [e.g., emerimicin-(1–9) benzyl ester], the same observation for 3_{10}-helices is infrequent (for a discussion of helical packing, see ref. 51). Packing within a particular layer may be parallel, but alternate layers pack in an antiparallel fashion as seen in a decamer, Boc-Aib-Val-Aib-Aib-Val-Val-Val-Aib-Val-Aib-OMe, by Karle *et al.* (21). In reality, the helices are packed antiparallel in a hexagonal array with four antiparallel and two parallel nearest neighbors (28). Two of the six surrounding helices in the hexagonal array must run parallel to the center helix, and this would give rise to the sheet of parallel helices often reported. In the case of emerimicin-(2–9), the packing of the 3_{10}-helices is even more unusual, with alternate layers of parallel helices orthogonally packed. A diagram in the paper (24) is misleading, showing the only view in which the projection of the orthogonal arrangement appears antiparallel. This absence of parallel packing for 3_{10}-helices, with one exception (25), substantiates the enhanced electrostatic interactions discussed above.

Clearly, segment 2–9 of emerimicin has a similar potential for assuming either the α- or the 3_{10}-helical conformation. It is possible that an interconversion between these helical forms may be responsible, in part, for the sensitivity to voltage seen with pores formed by peptaibol antibiotics such as alamethicin (52, 53). The work of Tosteson *et al.* (54) showing that a 22-residue segment of the S4 repeat of the sodium channel is capable of forming voltage-gated channels suggests that the 3_{10}-helix may be the active form, as this form maximizes the hydrophobic moment of this sequence (E.E.H. and G.R.M., unpublished data).

CONCLUSIONS

The conformations assumed by peptides containing multiple α,α-dialkyl amino acids are limited to several dominant families. The choice between α-helix and 3_{10}-helix depends on peptide length, environment, and size and distribution of amino acid side chains. Once a critical length of seven to eight residues is reached in solution, the α-helix is favored, especially in more polar solvents. In the crystal, the electrostatic interactions between the dipoles associated with the aligned amide bonds dominate, leading to antiparallel helices that are associated head-to-tail. If possible, the 3_{10}-helix is preferred due to its reduced radius and closer packing in a hexagonal antiparallel array. As the side-chain bulk is increased, the reduced radius of the 3_{10}-helix becomes proportionately less of a factor and the inherent stability of the α-helix predominates. Given sufficient bulk in the side chains, other interactions can dominate and parallel arrangement of the helices becomes possible as is seen in the crystal structure of emerimicin-(1–9). Sequence-dependent perturbations of these general concepts governing helix preference complicate the interpretation of the results for particular sequences. These factors govern the helical preference of peptides containing multiple α,α-dialkyl amino acids.

We thank Drs. Denise Beusen, John Clark, and Jim Dunbar for their support and criticisms of this work. This research was supported in part by National Institutes of Health Grants GM32812 (G.D.S.), GM24482 (G.R.M.), and GM33918 (G.R.M.). Two of us

(J.Z. and M.T.L.) acknowledge financial support for part of this work from the Polish Academy of Sciences (Grant CPBP 01.13.2.5).

1. Marshall, G. R. & Bosshard, H. E. (1972) *Circ. Res.* **30/31,** Suppl. II, 143–150.
2. Marshall, G. R. (1971) *Intra-Science Chem. Rep.* **5,** 305–316.
3. Burgess, A. W. & Leach, S. J. (1973) *Biopolymers* **12,** 2599–2605.
4. Pletnev, V. Z., Gromov, E. P. & Popov, E. M. (1973) *Khim. Prir. Soedin.*, 224–229.
5. Prasad, B. V. V. & Sasisekharan, V. (1979) *Macromolecules* **12,** 1107–1110.
6. Paterson, Y., Rumsey, S. M., Benedetti, E., Nemethy, G. & Scheraga, H. A. (1981) *J. Am. Chem. Soc.* **103,** 2947–2955.
7. Smith, G. D., Pletnev, V. Z., Duax, W. L., Balasubramanian, T. M., Bosshard, H. E., Czerwinski, E. W., Kendrick, N. E., Mathews, F. S. & Marshall, G. R. (1981) *J. Am. Chem. Soc.* **103,** 1493–1501.
8. Pandey, R. C., Cook, J. C., Jr., & Rinehart, K. C., Jr. (1977) *J. Am. Chem. Soc.* **99,** 5205–5206.
9. Prasad, B. V. V. & Balaram, P. (1984) *Crit. Rev. Biochem.* **16,** 307–348.
10. Marshall, G. R. (1982) in *Chemical Regulation of Biological Mechanisms*, eds. Creighton, A. M. & Turner, S. (Royal Society of Chemistry, London), pp. 279–292.
11. Marshall, G. R., Clark, J. D., Dunbar, J. B., Jr., Smith, G. D., Zabrocki, J., Redlinski, A. S. & Leplawy, M. T. (1988) *Int. J. Peptide Protein Res.* **32,** 544–555.
12. Benedetti, E., Barone, V., Bavoso, A., Di Blasio, B., Lelj, F., Pavone, V., Pedone, C., Bonora, G. M., Toniolo, C., Leplawy, M. T., Kaczmarek, K. & Redlinski, A. (1988) *Biopolymers* **27,** 357–371.
13. Fox, R. O., Jr., & Richards, F. M. (1982) *Nature (London)* **300,** 325–330.
14. Esposito, G., Carver, J. A., Boyd, J. & Campbell, I. D. (1987) *Biochemistry* **26,** 1043–1050.
15. Toniolo, C., Bonora, G. M., Bavoso, A., Benedetti, E., Di Blasio, B., Pavone, V. & Pedone, C. (1983) *Biopolymers* **22,** 205–215.
16. Bosch, R., Jung, G., Schmitt, H. & Winter, W. (1985) *Biopolymers* **24,** 961–978.
17. Bosch, R., Jung, G., Schmitt, H. & Winter, W. (1985) *Biopolymers* **24,** 979–999.
18. Karle, I. L., Sukumar, M. & Balaram, P. (1986) *Proc. Natl. Acad. Sci. USA* **83,** 9284–9288.
19. Karle, I. L., Flippen-Anderson, J., Sukumar, M. & Balaram, P. (1987) *Proc. Natl. Acad. Sci. USA* **84,** 5087–5091.
20. Karle, I. L., Flippen-Anderson, J., Uma, K. & Balaram, P. (1988) *Proc. Natl. Acad. Sci. USA* **85,** 299–303.
21. Karle, I. L., Flippen-Anderson, J. L., Uma, K., Balaram, H. & Balaram, P. (1989) *Proc. Natl. Acad. Sci. USA* **86,** 765–769.
22. Karle, I. L., Flippen-Anderson, J. L., Uma, K. & Balaram, P. (1988) *Int. J. Peptide Protein Res.* **32,** 536–543.
23. Karle, I. L., Flippen-Anderson, J. L., Sakumar, M. & Balaram, P. (1988) *Int. J. Peptide Protein Res.* **31,** 567–576.
24. Toniolo, C., Bonora, G. M., Bavoso, A., Benedetti, E., Di Blasio, B., Pavone, V. & Pedone, C. (1985) *J. Biomol. Struc. Dynamics* **3,** 585–598.
25. Bavoso, A., Benedetti, E., Di Blasio, B., Pavone, V., Pedone, C., Toniolo, C., Bonora, G. M., Formaggio, F. & Crisma, M. (1988) *J. Biomol. Struc. Dynamics* **5,** 803–817.
26. Francis, A. K., Iqbal, M., Balaram, P. & Vijayan, M. (1982) *J. Chem. Soc. Perkin Trans. 2*, 1235–1239.
27. Francis, A. K., Iqbal, M., Balaram, P. & Vijayan, M. (1983) *FEBS Lett.* **155,** 230–232.
28. Francis, A. K., Vijayakumar, E. K. S., Balaram, P. & Vijayan, M. (1985) *Int. J. Peptide Protein Res.* **26,** 214–223.
29. Bavoso, A., Benedetti, E., Di Blasio, B., Pavone, V., Pedone, C., Toniolo, C. & Bonora, G. M. (1986) *Proc. Natl. Acad. Sci. USA* **83,** 1988–1992.
30. Blessing, R. H. (1987) *Crystallogr. Rev.* **1,** 3–58.
31. Abrahams, S. C. & Keve, E. V. (1971) *Acta Crystallogr. A* **27,** 157–165.
32. Iijima, H., Dunbar, J. B., Jr., & Marshall, G. R. (1987) *Proteins Struct. Funct. Genet.* **2,** 330–339.
33. Weiner, S. J., Kollman, P. A., Case, D. A., Singh, U. C., Ghio, C., Alagona, G., Profeta, S. & Weiner, P. (1984) *J. Am. Chem. Soc.* **106,** 765–784.
34. Barlow, D. J. & Thornton, J. M. (1988) *J. Mol. Biol.* **201,** 601–619.
35. Jorgensen, W. L. & Swenson, C. J. (1985) *J. Am. Chem. Soc.* **107,** 569–578.
36. Jorgensen, W. L. & Tirado-Rives, J. (1988) *J. Am. Chem. Soc.* **110,** 1657–1666.
37. Davies, M. M., Jones, P., Patnaik, D. & Moelwyn-Hughes, E. A. (1951) *Trans. Chem. Soc.*, 278.
38. Vijayakumar, E. K. S. & Balaram, P. (1983) *Tetrahedron* **39,** 2725–2731.
39. Balaram, H., Sukumar, M. & Balaram, P. (1986) *Biopolymers* **25,** 2209–2223.
40. Presta, L. G. & Rose, G. D. (1988) *Science* **240,** 1632–1641.
41. Richardson, J. S. & Richardson, D. C. (1988) *Science* **240,** 1632–1641.
42. Malcolm, B. R. (1977) *Biopolymers* **16,** 2591–2592.
43. Malcolm, B. R. (1983) *Biopolymers* **22,** 319–322.
44. Sorensen, R. A., Liau, W. B., Kesner, L. & Boyd, R. H. (1988) *Macromolecules* **21,** 200–208.
45. Hol, W. G. J. & De Maeyer, M. C. H. (1984) *Biopolymers* **23,** 809–817.
46. Furois-Corbin, S. & Pullman, A. (1986) *Biochim. Biophys. Acta* **860,** 165–177.
47. Furois-Corbin, S. & Pullman, A. (1987) *Biochim. Biophys. Acta* **902,** 31–45.
48. Toniolo, C., Bonora, G. M., Benedetti, E., Bavoso, A., Di Blasio, B., Pavone, V. & Pedone, C. (1983) *Biopolymers* **22,** 1335–1356.
49. Okuyama, K., Tanaka, N., Doi, M. & Narita, M. (1988) *Bull. Chem. Soc. Jpn.* **61,** 3115–3120.
50. Bonora, G. M., Toniolo, C., Di Blasio, B., Pavone, V., Pedone, C., Benedetti, E., Lingham, I. & Hardy, P. (1984) *J. Am. Chem. Soc.* **106,** 8152–8156.
51. Karle, I. L. (1989) *Biopolymers* **28,** 1–14.
52. Hall, J. E., Vodyanoy, I., Balasubramanian, T. M. & Marshall, G. R. (1984) *Biophys. J.* **45,** 233–247.
53. Menestrina, G., Voges, K. P., Jung, G. & Boheim, G. (1986) *J. Membr. Biol.* **93,** 111–132.
54. Tosteson, M. T., Auld, D. S. & Tosteson, D. C. (1989) *Proc. Natl. Acad. Sci. USA* 86, 707–710.